

Supporting information for

Investigation of SCO Property - Structural Relationships in a Family of Mononuclear Fe(II) Complexes

Xiu-Qin Chen,^a You-De Cai,^a Yi-Shan Ye,^a Ming-Liang Tong^b and Xin Bao^{a, c*}

[a] School of Chemical Engineering, Nanjing University of Science and Technology, 210094 Nanjing, P. R. China

E-mail: baox199@126.com

[b] School of Chemistry, Sun Yat-Sen University, 510275, Guangzhou, P. R. China

[c] State Key Laboratory of Coordination Chemistry, Coordination Chemistry Institute, School of Chemistry and Chemical Engineering, Nanjing University, Nanjing 210093, P. R. China

Experimental Section	S3
Physical characterization	S5
Figure S1. View of the molecular structures of the Fe(II) complex in 1 – 3 at 123 K.	S6
Figure S2. View of the molecular structures of the Fe(II) complex in 4 – 6 at 123 K (4a at 173 K).....	S6
Figure S3. Differential scanning calorimetry (DSC) curves of 6	S7
Figure S4. Take ^{2Me} L _{quinoline} as an example, showing tetradentate ligands possessing two amine sites and two pyridine/pyrazine in <i>mer</i> positions.	S7
Figure S5. Packing diagrams showing the 2D flat layers (top) and arrangement between adjacent flat layers(bottom) in 6 (left) and [Fe(^{2Me} L _{pz})(NCBH ₃) ₂] (right).....	S8
Figure S6. IR spectra for 1, 2 and 3	S9
Figure S7. IR spectra for 4a, 4b, 5 and 6	S9
Figure S8. Experimental and simulated PXRD patterns of 1	S10
Figure S9. Experimental and simulated PXRD patterns of 2	S10
Figure S10. Experimental and simulated PXRD patterns of 3	S11
Figure S11. Experimental and simulated PXRD patterns of 4a	S11
Figure S12. Experimental and simulated PXRD patterns of 4b	S12
Figure S13. Experimental and simulated PXRD patterns of 5	S12
Figure S14. Experimental and simulated PXRD patterns of 6	S13
Figure S15. Thermogravimetric analysis (TGA) curves for 1, 2 and 3	S13
Figure S16. Thermogravimetric analysis (TGA) curves for 4a, 4b, 5 and 6	S14
Figure S17. Comparison of the optical spectra at room temperature for the [NiL(NCS) ₂] complexes	S15
Figure S18. Comparison of the optical spectra at room temperature for the [Ni(^{Dibenzyl} L)(NCE) ₂].....	S15
Table S1. Crystal data and refinement details for 1, 2 and 3 , respectively.	S16
Table S2. Selected bond lengths and structural parameters for 1, 2 and 3 , respectively.....	S17
Table S3. Crystal data and refinement details for 4a, 4b, 5 and 6 , respectively.	S18
Table S4. Selected bond lengths and structural parameters for 4a, 4b, 5 and 6 , respectively.	S19
Table S5. The tetradentate ligand (L) and the spin-state of [FeL(NCE) ₂] discussed.	S20
References	S21

Experimental Section

General. All reagents obtained from commercial sources were used without further purification. Safety Note: Perchlorate salts are potentially explosive, and caution should be taken when dealing with such materials.

Synthetic Procedures.

Synthesis of N,N' -Dimethyl- N,N' -bis-(quinoline-2-ylmethyl)ethane-1,2-diamine ($^{2Me}L_{quinoline}$) and N,N' -Dibenzyl-bis-(pyridin-2-ylmethyl) ethane-1,2-diamine ($^{Dibenzyl}L$).

The ligands $^{2Me}L_{quinoline}$ ligand and $^{Dibenzyl}L$ were synthesized according to the reported references [1] [2].

Synthesis of $[Fe(^{2Me}L_{quinoline})(NCS)_2](1)$. To a 20 mL solution of $^{2Me}L_{quinoline}$ (0.037 g, 0.1 mmol) in MeOH were added 0.036 g (0.1 mmol) of $Fe(ClO_4)_2 \cdot 6H_2O$ and 0.018 g (0.2 mmol) of KSCN. The resulting reaction mixture was stirred for 0.5 h, and the yellow precipitate was filtered. Recrystallization from hot MeCN gave yellow rhombus crystals in 60% yield. IR (KBr, cm^{-1}): 3108 (w), 3083 (w), 3012 (w), 2975 (w), 2921 (w), 2887 (w), 2811 (w), 2054 (s, $C \equiv N$), 1598 (m, $C=C$), 1567 (w), 1510 (m), 1465 (m), 1434 (m), 1299 (m), 1211 (w), 1183 (w), 1143 (w), 1117 (w), 1074 (m), 1018 (w), 983 (m), 962 (m), 826 (m), 751 (m), 704 (m), 630 (m), 602 (w). Elemental analyses. Calcd: C, 57.56; H, 4.83; N, 15.49. Found: C, 57.33; H, 4.77; N, 15.41.

Synthesis of $[Fe(^{2Me}L_{quinoline})(NCSe)_2](2)$. To a 20 mL solution of $^{2Me}L_{quinoline}$ (0.037 g, 0.1 mmol) in MeOH were added 0.036 g (0.1 mmol) of $Fe(ClO_4)_2 \cdot 6H_2O$ and 0.028 g (0.2 mmol) of KSeCN. The resulting reaction mixture was stirred for 0.5 h, and the yellow precipitate was filtered. Recrystallization from hot MeCN gave green slice crystals in 55% yield. IR (KBr, cm^{-1}): 3110 (w), 3084 (w), 3010 (w), 2976 (w), 2923 (w), 2889 (w), 2865 (w), 2812 (w), 2057 (s, $C \equiv N$), 1598 (m, $C=C$), 1567 (w), 1512 (m), 1466 (w), 1431 (w), 1345 (w), 1300 (w), 1184 (w), 1143 (w), 1078 (m), 1018 (w), 987 (w), 962 (w), 826 (m), 781 (w), 753 (m), 635 (w), 603 (w). Elemental analyses. Calcd: C, 49.08; H, 4.12; N, 13.21. Found: C, 49.26; H, 4.12; N, 13.25.

Synthesis of $[Fe(^{2Me}L_{quinoline})(NCBH_3)_2](3)$. To a 20 mL solution of $^{2Me}L_{quinoline}$ (0.037 g, 0.1 mmol) in MeOH were added 0.036 g (0.1 mmol) of $Fe(ClO_4)_2 \cdot 6H_2O$ and 0.012 g (0.2 mmol) of $NaNCBH_3$. The resulting reaction mixture was stirred for 0.5 h, and the yellow precipitate was filtered. Recrystallization from hot MeOH gave green rhombus crystals in 50% yield. IR (KBr, cm^{-1}): 3367 (m), 3008 (w), 2976 (w), 2931 (w), 2384 (w), 2344 (m), 2267 (w), 2217 (w), 2181 (s, $C \equiv N$), 1599 (m, $C=C$), 1573 (w), 1510 (m), 1465 (m), 1430 (w), 1371 (w), 1340 (w), 1295 (m), 1211 (w), 1188 (w), 1112 (m), 1072 (m), 983 (w), 965 (w), 831 (m), 777 (m), 745 (m), 634 (m). Elemental analyses. Calcd: C,

61.71; H, 6.37; N, 16.61. Found: C, 61.33; H, 6.28; N, 16.57.

Synthesis of $[\text{Fe}(\text{DibenzylL})(\text{NCS})_2](\mathbf{4a})$. To a 20 mL solution of DibenzylL (0.042 g, 0.1 mmol) in MeOH were added 0.036 g (0.1 mmol) of $\text{Fe}(\text{ClO}_4)_2 \cdot 6\text{H}_2\text{O}$ and 0.018 g (0.2 mmol) of KSCN. The resulting reaction mixture was stirred for 0.5 h, and the yellow precipitate was filtered. Recrystallization from hot MeOH and DMF (ratio 10:1) and then kept at 4°C give yellow triangle crystals in 60% yield. IR (KBr, cm^{-1}): 3440 (w), 3063 (w), 3024 (w), 2959 (w), 2882 (w), 2060 (s, $\text{C}\equiv\text{N}$), 1601 (m, $\text{C}=\text{C}$), 1569 (w), 1436 (m), 1338 (w), 1295 (w), 1201 (w), 1155 (w), 1062 (m), 1016(w), 952 (m), 852 (w), 801 (w), 769 (m), 749 (m), 704 (m), 656 (w), 611 (w), 574 (w). Elemental analyses. Calcd: C, 60.60; H, 5.09; N, 14.13. Found: C, 60.67; H, 5.16; N, 14.39.

Synthesis of $[\text{Fe}(\text{DibenzylL})(\text{NCS})_2](\mathbf{4b})$. To a 20 mL solution of DibenzylL (0.042 g, 0.1 mmol) in MeCN were added 0.036 g (0.1 mmol) of $\text{Fe}(\text{ClO}_4)_2 \cdot 6\text{H}_2\text{O}$ and 0.018 g (0.2 mmol) of KSCN. The resulting reaction mixture was stirred for 0.5 h, and the yellow solution was evaporated in one day. Rectangular prism yellow crystals were obtained in 60% yield. IR (KBr, cm^{-1}): 3453 (m), 3046 (w), 2955 (w), 2883 (w), 2060 (s, $\text{C}\equiv\text{N}$), 1602 (m, $\text{C}=\text{C}$), 1565 (w), 1440 (m), 1338 (w), 1294 (w), 1254 (w), 1206 (w), 1153 (w), 1064 (m), 1015(w), 953 (m), 848 (w), 746 (m), 706 (m), 610 (w), 572 (w). Elemental analyses. Calcd: C, 60.60; H, 5.09; N, 14.13. Found: C, 60.63; H, 5.09; N, 14.43.

Synthesis of $[\text{Fe}(\text{DibenzylL})(\text{NCSe})_2](\mathbf{5})$. To a 20 mL solution of DibenzylL (0.042 g, 0.1 mmol) in MeCN were added 0.036 g (0.1 mmol) of $\text{Fe}(\text{ClO}_4)_2 \cdot 6\text{H}_2\text{O}$ and 0.028 g (0.2 mmol) of KSeCN . The resulting reaction mixture was stirred for 0.5 h, and the dark yellow solution was evaporated in one day. Strip yellow crystals were obtained in 55% yield. IR (KBr, cm^{-1}): 3450 (m), 3056 (w), 3021(w), 2948 (w), 2902 (w), 2060 (s, $\text{C}\equiv\text{N}$), 1604 (m, $\text{C}=\text{C}$), 1572 (w), 1482(w), 1443 (m), 1349 (w), 1289 (w), 1201 (w), 1150 (w), 1099 (w), 1057 (m), 1020 (w), 956 (w), 931 (m), 854 (w), 793 (w), 756 (m), 704 (m), 654 (w), 608 (w) , 578 (w). Elemental analyses. Calcd: C, 52.34; H, 4.39; N, 12.21. Found: C, 52.42; H, 4.46; N, 12.48.

Synthesis of $[\text{Fe}(\text{DibenzylL})(\text{NCBH}_3)_2](\mathbf{6})$. To a 20 mL solution of DibenzylL (0.042 g, 0.1 mmol) in MeCN were added 0.036 g (0.1 mmol) of $\text{Fe}(\text{ClO}_4)_2 \cdot 6\text{H}_2\text{O}$ and 0.012 g (0.2 mmol) of NaNCBH_3 . The resulting reaction mixture was stirred for 0.5 h, and the light yellow solution was evaporated in three days. Hexagon green emerald crystals were obtained in 50% yield. IR (KBr, cm^{-1}): 3435 (m), 3062 (w), 3031 (w), 2956 (w), 2907 (w), 2393 (m), 2348 (m), 2316 (m), 2268 (w), 2184 (s, $\text{C}\equiv\text{N}$), 1605 (m, $\text{C}=\text{C}$), 1574 (w), 1487 (w), 1448 (m), 1345 (w), 1295 (w), 1205 (w), 1118 (m), 1062 (m), 1020 (w), 854 (w), 797 (w), 767 (m), 706 (m), 610 (w), 582 (w), 483 (w), 455 (w). Elemental analyses. Calcd: C, 64.56; H, 6.50; N, 15.06. Found: C, 64.70; H, 6.55; N, 15.40.

Physical characterization

Magnetic susceptibility measurements were recorded with a Quantum Design PPMS-9, operating with an applied field of 1.0 T at temperatures between 10 and 300 K at rate of 2 K min⁻¹. **Elemental analyses** were performed using an Elementar Vario EL Elemental Analyser. **The IR spectra** were recorded using KBr discs in the range of 4000–500 cm⁻¹ with a Perkin-Elmer Spectrum. **DSC** measurement was performed on a METTLER TOLEDO DSC823 instrument under a nitrogen atmosphere at a scan rate of 5 K min⁻¹ in both heating and cooling modes. **PXRD** patterns were recorded on a D8 ADVANCE X-ray diffractometer (CuK α radiation, $\lambda = 0.154056$ nm). **TG** curves were recorded on a Mettler-Toledo TGA / SDTA851^e thermoanalyzer by filling the sample into alumina crucibles under a nitrogen atmosphere within the temperature range of 323–1073 K at a heating rate of 10 K min⁻¹.

Single crystal X-ray diffraction. Single-crystal X-ray data were collected on a Bruker D8 Quest diffractometer using graphite monochromated Mo-K α radiation ($\lambda = 0.71073$ Å). A multi-scan absorption correction was performed (SADABS, Bruker, 2016). The structures were solved using direct method (SHELXS) and refined by full-matrix least-squares on F^2 using SHELXL^[2] under the graphical user interface of Olex2.^[3] Non-hydrogen atoms were refined anisotropically, and hydrogen atoms were placed in calculated positions refined using idealized geometries (riding model) and assigned fixed isotropic displacement parameters. CCDC 1916633–1916640 contain the supplementary crystallographic data for this paper. These data can be obtained free of charge from The Cambridge Crystallographic Data Centre via www.ccdc.cam.ac.uk/data_request/cif.

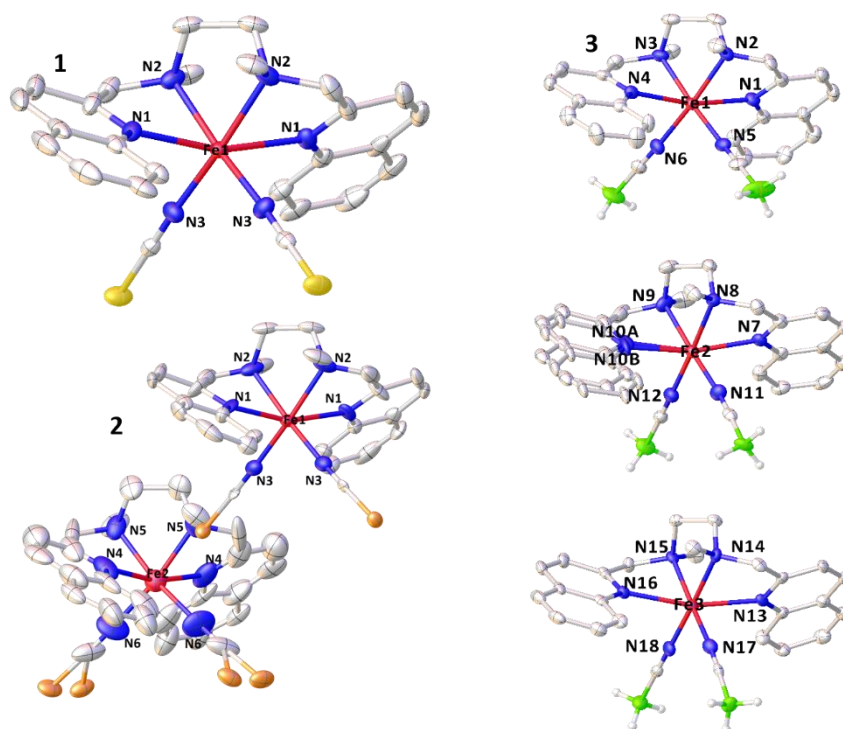


Figure S1. View of the molecular structures of the Fe(II) complex in **1** – **3** at 123 K. Thermal ellipsoids are presented at 50% probability. Color code: Fe, red; C, gray; H, white; S, yellow; Se, orange; B, green; N, blue. H atoms in the tetradentate ligand were omitted for clarity.

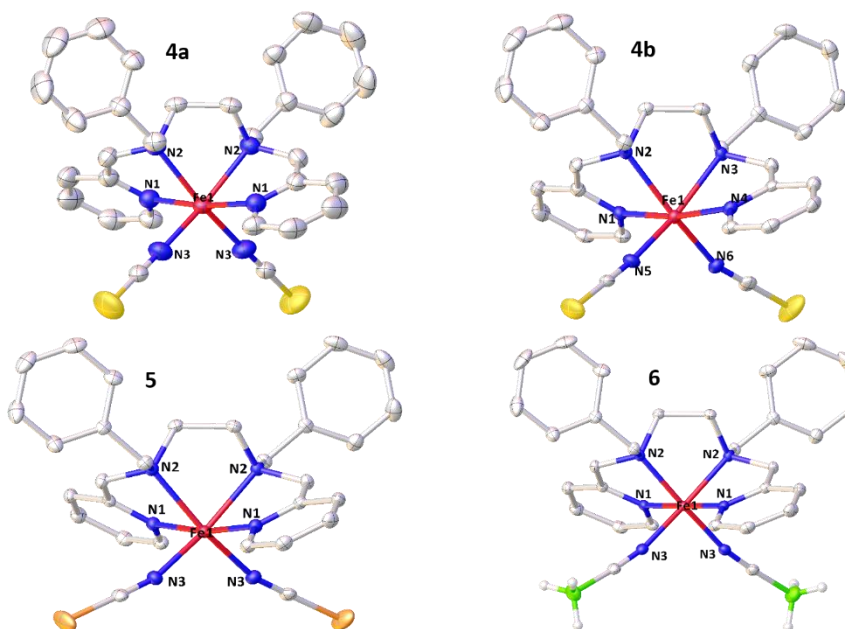


Figure S2. View of the molecular structures of the Fe(II) complex in **4** – **6** at 123 K (**4a** at 173 K). Thermal ellipsoids are presented at 50% probability. Color code: Fe, red; C, gray; H, white; S, yellow; Se, orange; B, green; N, blue. H atoms in the tetradentate ligand were omitted for clarity.

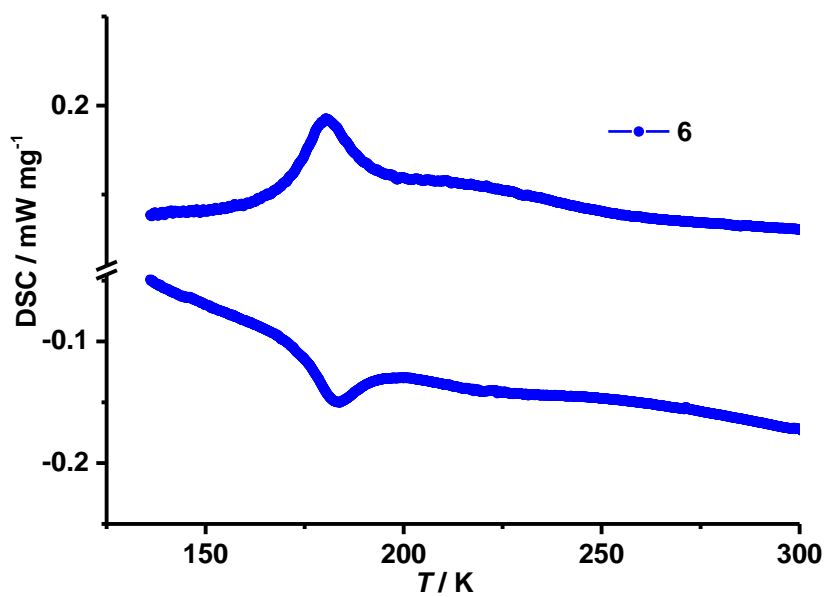


Figure S3. Differential scanning calorimetry (DSC) curves of **6** in the heating and cooling modes at a sweep rate of 5 K min⁻¹.

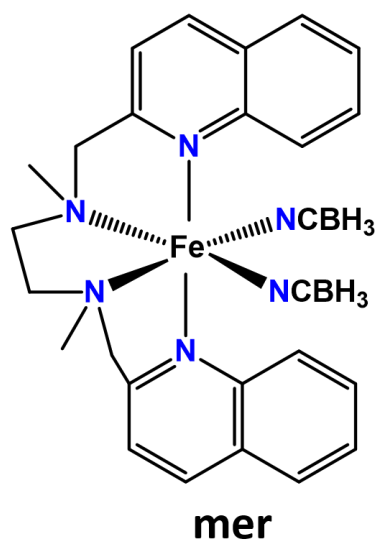


Figure S4. Take ^{2Me}L_{quinoline} as an example, showing tetradentate ligands possessing two amine sites and two pyridine/pyrazine in *mer* positions.

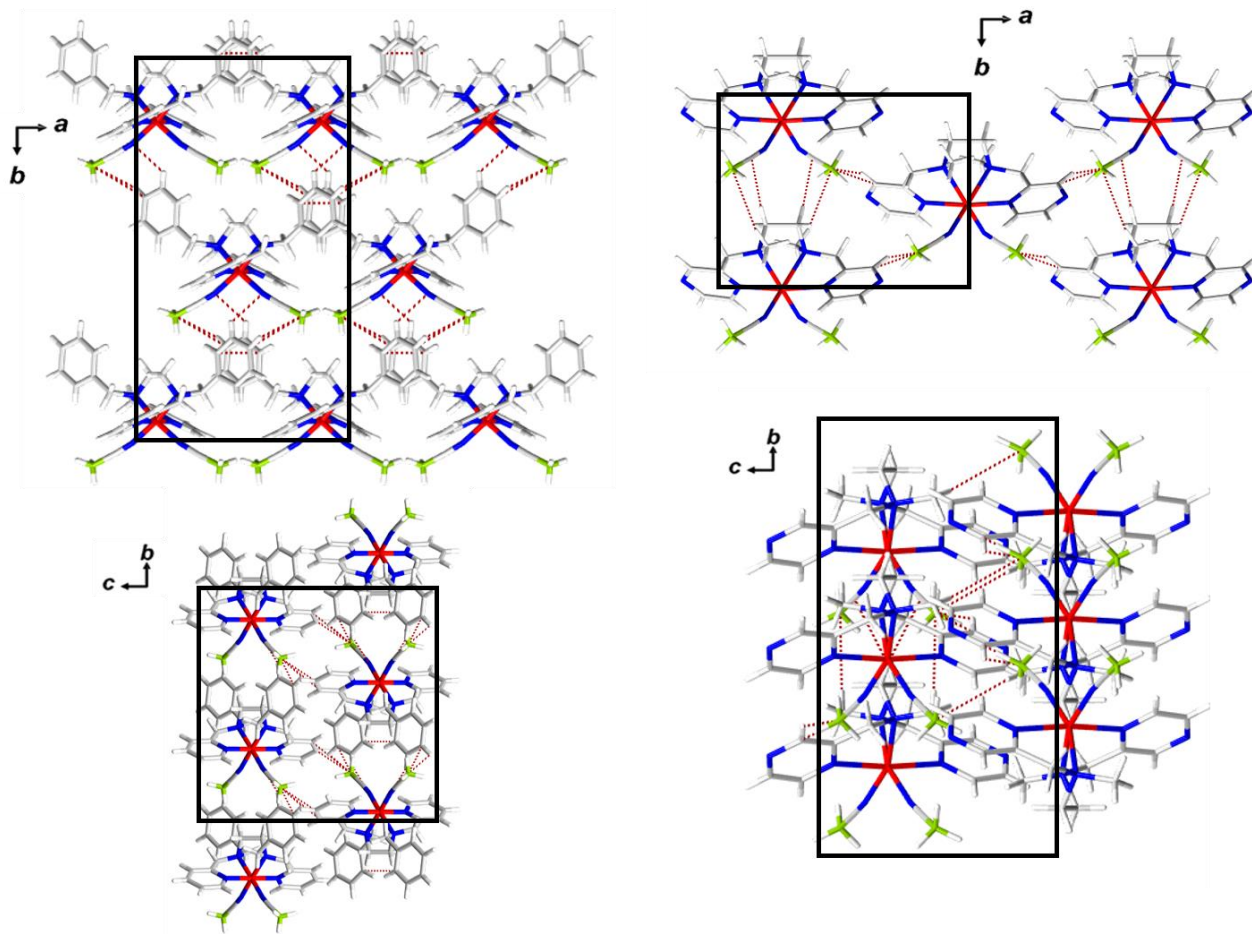


Figure S5. Packing diagrams showing the 2D flat layers (top) and arrangement between adjacent flat layers (bottom) in **6** (left) and $[\text{Fe}^{(2\text{MeLpz})}(\text{NCBH}_3)_2]$ (right). The supramolecular interactions are shown in red dotted lines.

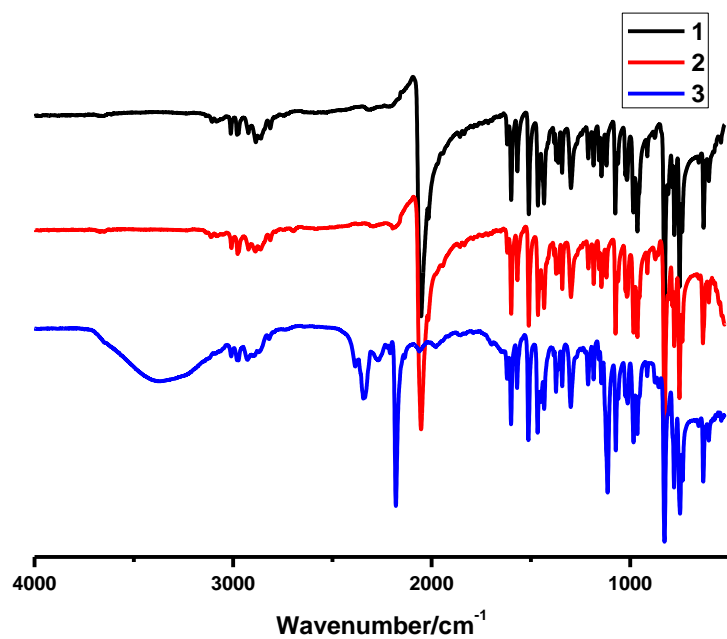


Figure S6. IR spectra for **1** (black), **2** (red) and **3** (blue) in the region of 4000–500 cm⁻¹ at room temperature.

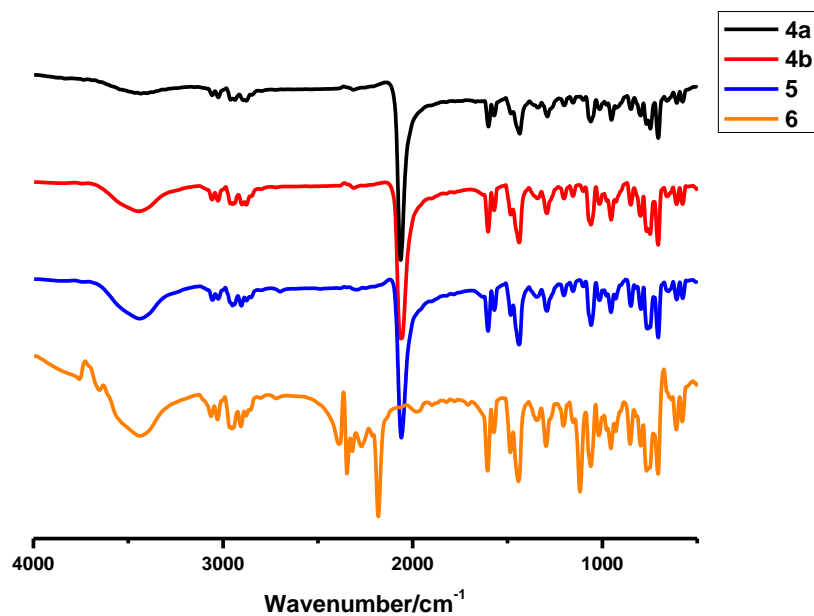


Figure S7. IR spectra for **4a** (black), **4b** (red), **5** (blue) and **6** (orange) in the region of 4000–500 cm⁻¹ at room temperature.

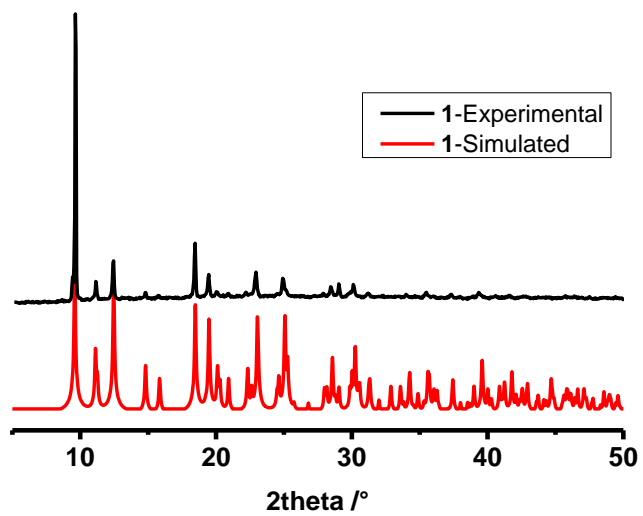


Figure S8. Experimental and simulated PXR D patterns of 1.

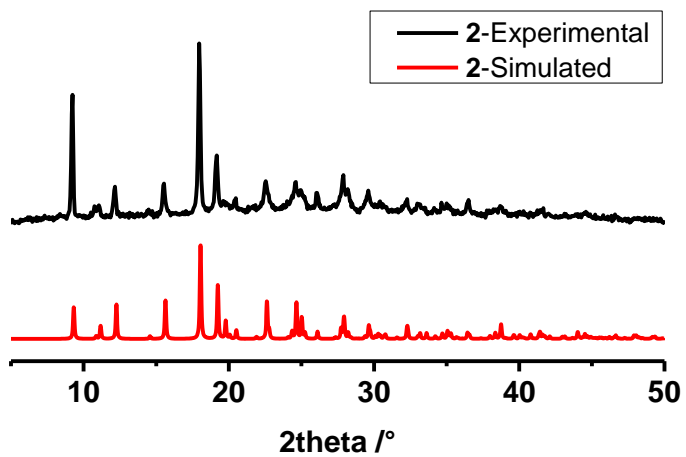


Figure S9. Experimental and simulated PXR D patterns of 2.

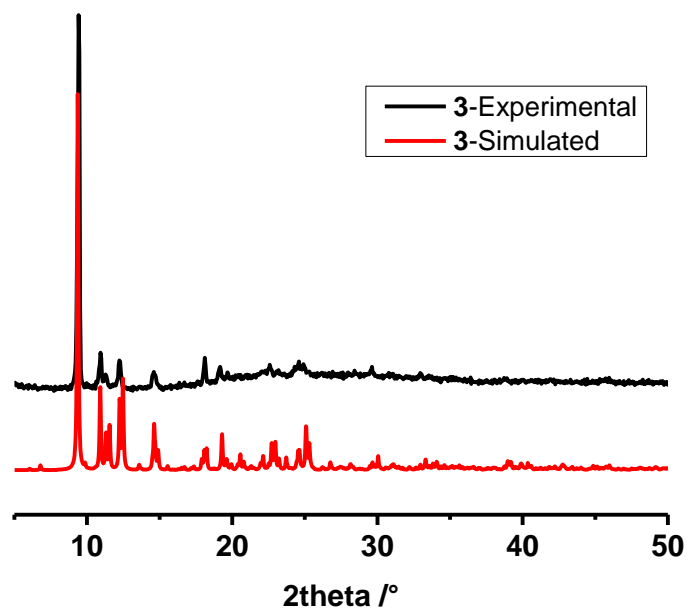


Figure S10. Experimental and simulated PXR D patterns of **3**.

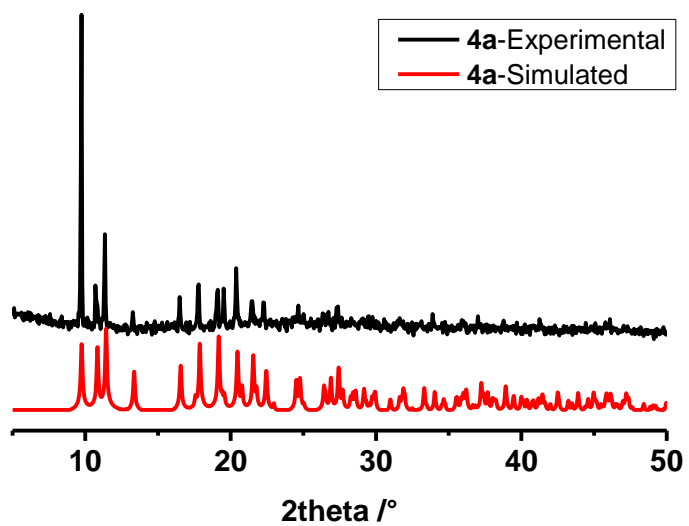


Figure S11. Experimental and simulated PXR D patterns of **4a**.

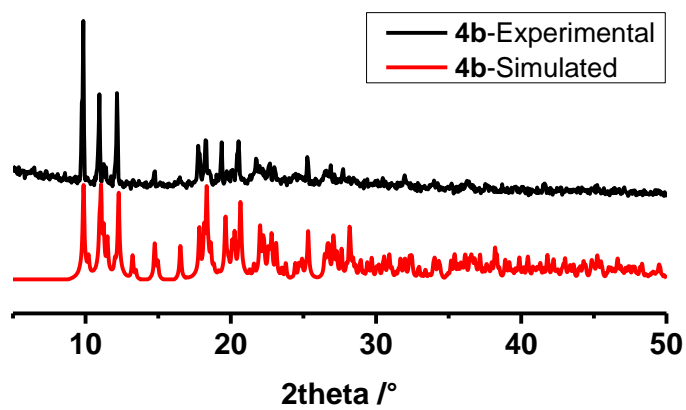


Figure S12. Experimental and simulated PXRD patterns of **4b**.

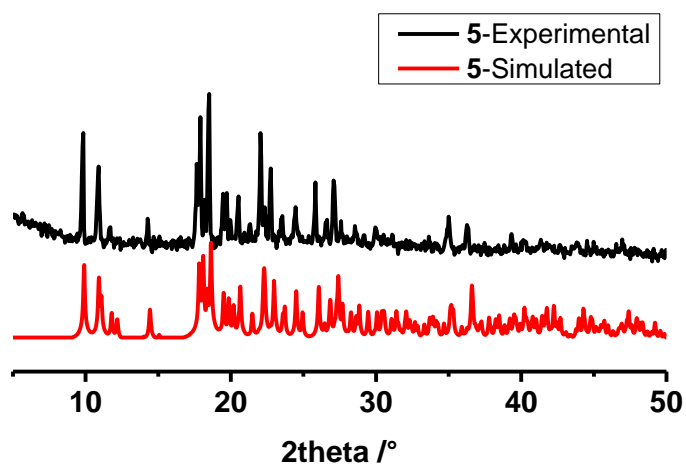


Figure S13. Experimental and simulated PXRD patterns of **5**.

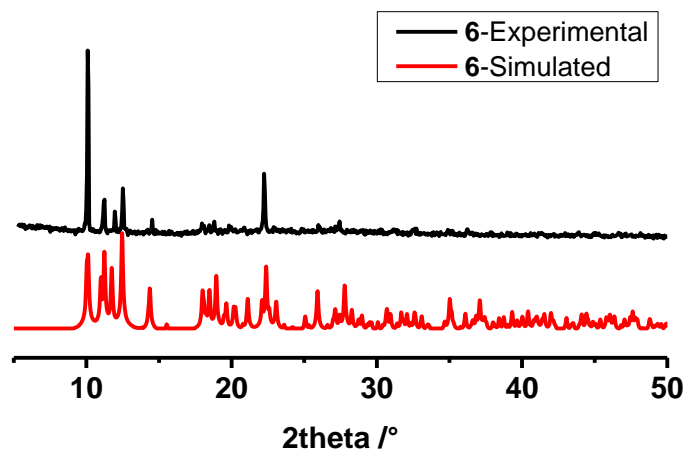


Figure S14. Experimental and simulated PXRD patterns of 6.

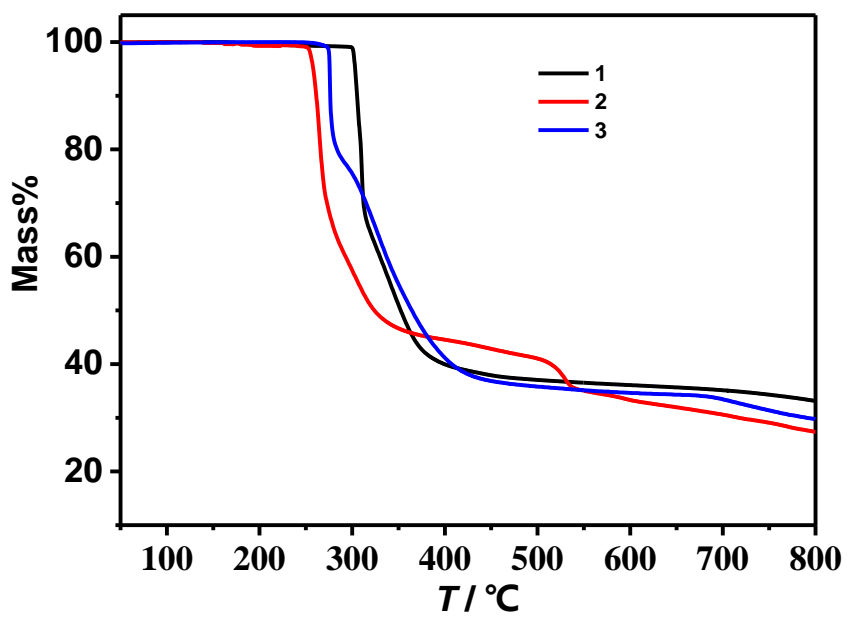


Figure S15. Thermogravimetric analysis (TGA) curves for 1, 2 and 3 from 50 to 800 °C at a 10 K min⁻¹ temperature rate under N₂ atmosphere.

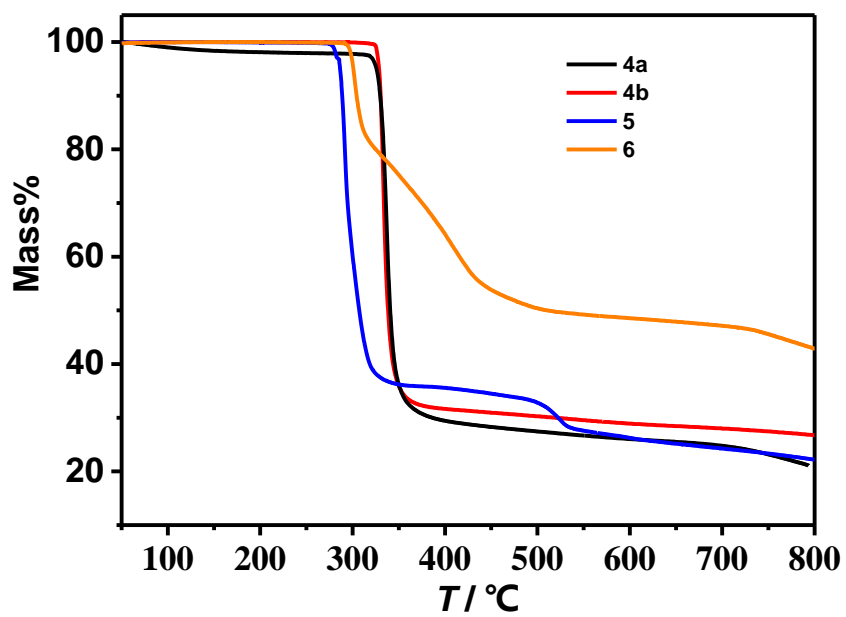


Figure S16. Thermogravimetric analysis (TGA) curves for **4a**, **4b**, **5** and **6** from 50 to 800 °C at a 10 K min⁻¹ temperature rate under N₂ atmosphere.

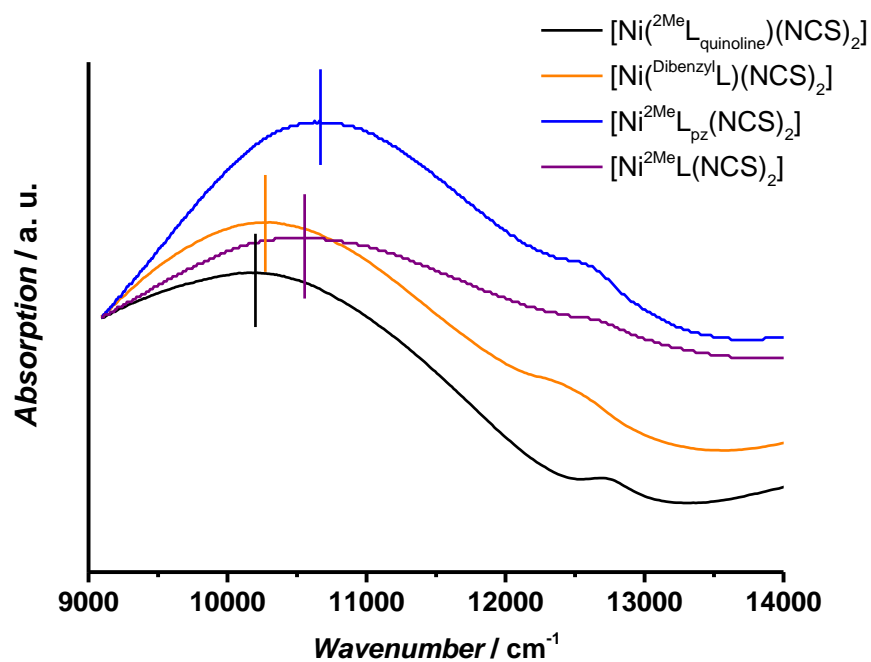


Figure S17. Comparison of the optical spectra at room temperature for the $[\text{NiL}(\text{NCS})_2]$ complexes ($\text{L} = \text{}^2\text{MeL}_{\text{quinoline}}$, DibenzylL , $\text{}^2\text{MeL}$ and $\text{}^2\text{MeL}_{\text{pz}}$) in the range of the d-d transition.

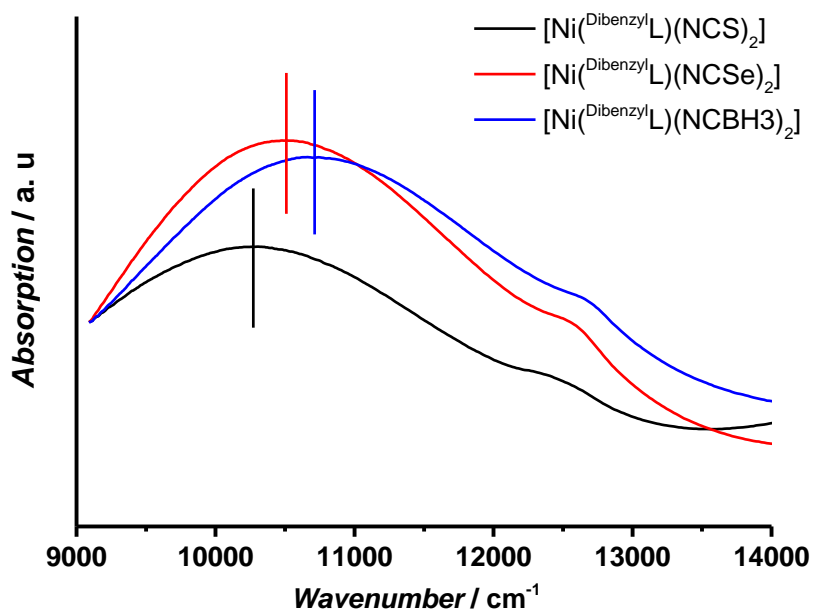


Figure S18. Comparison of the optical spectra at room temperature for the $[\text{Ni}(\text{DibenzylL})(\text{NCE})_2]$ complexes ($\text{E} = \text{S}$, Se and BH_3) in the range of the d-d transition.

Table S1. Crystal data and refinement details for **1**, **2** and **3**, respectively.

	1	2	3		
			Fe1	Fe2	Fe3
Temperature/K	123	123	123		
Empirical formula	C ₂₆ H ₂₆ FeN ₆ S ₂	C ₂₆ H ₂₆ FeN ₆ Se ₂	C ₇₈ H ₉₆ B ₆ Fe ₃ N ₁₈		
Formula weight /g mol ⁻¹	542.50	636.30	1518.13		
Crystal system	Orthorhombic	Orthorhombic	Monoclinic		
Space group	<i>Aea2</i>	<i>Pnc2</i>	<i>P2₁/c</i>		
<i>a</i> / Å	15.7067(15)	18.954(2)	23.453(3)		
<i>b</i> / Å	18.4252(18)	15.8604(19)	18.8759(18)		
<i>c</i> / Å	8.8199(8)	8.7328(9)	18.3057(18)		
β / °	—	—	101.887(3)		
Volume / Å ³	2552.5(4)	2625.2(5)	7930.1(15)		
<i>Z</i>	4	4	4		
ρ_{calc} / mg mm ⁻³	1.412	1.610	1.272		
μ / mm ⁻¹	0.781	3.374	0.596		
<i>F</i> (000)	1128.0	1272.0	3192.0		
Reflections collected	5765	26281	33206		
Independent reflections	2221	5319	15974		
<i>R</i> _{int}	<i>R</i> _{int} = 0.0416	<i>R</i> _{int} = 0.1308	<i>R</i> _{int} = 0.0957		
Goodness-of-fit on <i>F</i> ²	1.029	1.118	0.918		
Final <i>R</i> indexes ^a	<i>R</i> ₁ = 0.0335	<i>R</i> ₁ = 0.0847	<i>R</i> ₁ = 0.0621		
[<i>I</i> ≥ 2σ(<i>I</i>)]	<i>wR</i> ₂ = 0.0656	<i>wR</i> ₂ = 0.1618	<i>wR</i> ₂ = 0.1050		
Final <i>R</i> indexes	<i>R</i> ₁ = 0.0447	<i>R</i> ₁ = 0.1449	<i>R</i> ₁ = 0.1931		
[all data]	<i>wR</i> ₂ = 0.0698	<i>wR</i> ₂ = 0.1843	<i>wR</i> ₂ = 0.1488		
Largest diff. peak/hole / eÅ ⁻³	0.28/-0.54	1.10/-1.60	0.46/-0.56		

Table S2. Selected bond lengths and structural parameters for **1**, **2** and **3**, respectively.

	1	2		3		
		Fe1	Fe2	Fe1	Fe2	Fe3
T / K	123	123		123		
Spin state	HS	HS	HS	HS	HS	HS
Fe-N_{NCX} / Å	2.075(3)	2.058(15)	2.11(2)	2.115(4)	2.104(5)	2.102(4)
				2.105(4)	2.109(5)	2.110(4)
Fe-N_{pyridine} / Å	2.359(3)	2.338(14)	2.305(16)	2.321(4)	2.339(4)	2.355(4)
				2.328(4)	2.305 ^a	2.352(4)
Fe-N_{amine} / Å	2.228(3)	2.236(13)	2.225(16)	2.224(4)	2.222(4)	2.207(4)
				2.236(4)	2.228(4)	2.221(4)
Fe-N_{average} / Å	2.22	2.21	2.21	2.22	2.22	2.22
cis N-Fe-N / °	73.61(13)- 102.51(13)	74.1(5)- 102.7(5)	75.6(7)- 103.3(8)	74.12 (14)- 104.23(15)	72.3 (5)- 106.1(6)	74.33 (13)- 103.62(14)
trans N-Fe-N / °	162.95(15)- 171.68(13)	162.4(6)- 173.4(5)	165.6(10)- 171.1(8)	166.39(14)- 173.27(16)	163.2(5)- 174.67(16)	164.42(13)- 173.32(15)
Σ_{Fe} / °	85.6(7)	80(3)	91(4)	95.1(6)	89.05 ^a	88.5(6)
Θ	130.5(9)	134(4)	113(4)	130.3(7)	134.2 ^a	132.2(8)
N-C-X / °	179.4 (4)	177.8(13)	159.5 ^a	178.3(6)	178.1(6), 176.8(6)	179.7(6), 178.2(6)
Fe-N-C_{NCX} / °	176.2(3)	174.9(13)	178(2)	172.1(4), 171.2(4)	175.4(5), 174.6(4)	178.2(4), 175.5(4)

^a an average value was calculated due to the disorder of the ligand.

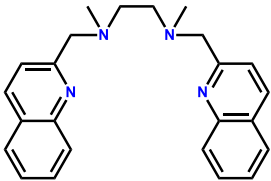
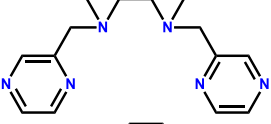
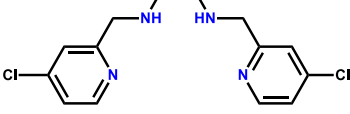
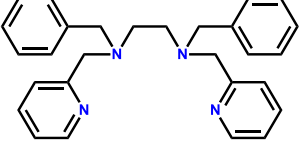
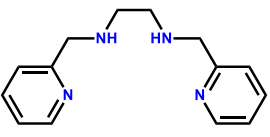
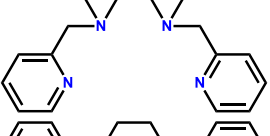
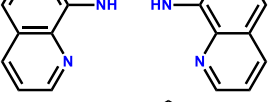
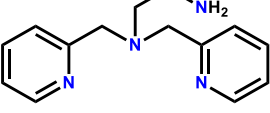
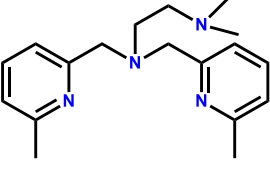
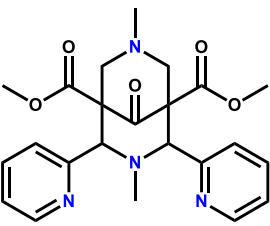
Table S3. Crystal data and refinement details for **4a**, **4b**, **5** and **6**, respectively.

	4a	4b	5	6	
Temperature / K	173	123	123	123	298
Empirical formula	C ₃₀ H ₃₀ FeN ₆ S ₂	C ₃₀ H ₃₀ FeN ₆ S ₂	C ₃₀ H ₃₀ FeN ₆ Se ₂	C ₃₀ H ₃₆ B ₂ FeN ₆	C ₃₀ H ₃₆ B ₂ FeN ₆
Formula weight / g mol⁻¹	594.57	594.59	688.37	558.12	558.12
Crystal system	Orthorhombic	Monoclinic	Monoclinic	Monoclinic	Monoclinic
Space group	<i>Fdd2</i>	<i>P2₁/c</i>	<i>C2/c</i>	<i>C2/c</i>	<i>C2/c</i>
<i>a</i> / Å	36.267(3)	8.9005(6)	9.1025(6)	9.0702(8)	9.1122(10)
<i>b</i> / Å	8.7886(5)	35.872(2)	17.8172(13)	17.6164(14)	18.0717(16)
<i>c</i> / Å	18.2623(11)	9.8596(6)	17.8861(12)	17.5397(15)	18.0770(18)
β / °	—	115.085(2)	92.747(3)	95.001(3)	93.971(4)
Volume / Å³	5820.9(7)	2851.0(3)	2897.5(3)	2791.9(4)	2969.6(5)
Z	8	4	4	4	4
ρ_{calc} / mg mm⁻³	1.357	1.3851	1.578	1.328	1.248
μ / mm⁻¹	0.692	0.706	3.064	0.571	0.537
<i>F</i>(000)	2480.0	1242.7	1384.0	1176.0	1176.0
Reflections collected	29295	16371	63101	15565	16864
Independent reflections	3321	5136	3326	3204	3422
<i>R</i>_{int}	<i>R</i> _{int} = 0.0342	<i>R</i> _{int} = 0.0685	<i>R</i> _{int} = 0.0360	<i>R</i> _{int} = 0.0353	<i>R</i> _{int} = 0.0439
Goodness-of-fit on <i>F</i>²	1.027	1.075	1.044	1.111	1.063
Final <i>R</i> indexes^a [<i>I</i> ≥ 2σ(<i>I</i>)]	<i>R</i> ₁ = 0.0241 <i>wR</i> ₂ = 0.0564	<i>R</i> ₁ = 0.0527 <i>wR</i> ₂ = 0.0850	<i>R</i> ₁ = 0.0270 <i>wR</i> ₂ = 0.0609	<i>R</i> ₁ = 0.0368 <i>wR</i> ₂ = 0.0777	<i>R</i> ₁ = 0.0409 <i>wR</i> ₂ = 0.0856
Final <i>R</i> indexes [all data]	<i>R</i> ₁ = 0.0292 <i>wR</i> ₂ = 0.0581	<i>R</i> ₁ = 0.0934 <i>wR</i> ₂ = 0.0959	<i>R</i> ₁ = 0.0320 <i>wR</i> ₂ = 0.0630	<i>R</i> ₁ = 0.0459 <i>wR</i> ₂ = 0.0802	<i>R</i> ₁ = 0.0633 <i>wR</i> ₂ = 0.0923
Largest diff. peak/hole / eÅ⁻³	0.28/-0.25	0.70/-0.77	0.73/-0.99	0.37/-0.45	0.19/-0.27

Table S4. Selected bond lengths and structural parameters for **4a**, **4b**, **5** and **6**, respectively.

	4a	4b	5	6	
<i>T</i> / K	173	123	123	123	298
Spin state	HS	HS	HS	LS	HS
Fe-N _{NcX} / Å	2.067(2)	2.074(3)	2.0820(15)	1.9479(15)	2.0990(18)
Fe-N _{pyridine} / Å	2.1728(18)	2.176(3)	2.1869(14)	1.9944(14)	2.1817(15)
Fe-N _{amine} / Å	2.2696(19)	2.275(3)	2.2660(14)	2.0620(14)	2.2635(15)
Fe-N _{average} / Å	2.17	2.17	2.17	2.00	2.18
<i>cis</i> N-Fe-N / °	76.14(7)- 103.39(12)	75.87(9)- 104.89(11)	75.93(5)- 104.68(8)	81.31 (6)- 98.33(6)	76.02(5)- 102.53(9)
<i>trans</i> N-Fe-N / °	163.39(7)- 172.40(11)	162.16(10)- 171.14(10)	162.68(5)- 170.57(8)	170.94(6)- 179.50(8)	163.97(6)- 171.17(8)
Σ Fe / °	77.2(3)	79.7(3)	79.8(2)	51.7(4)	75.9(3)
Θ	177.0(6)	221.6(8)	220.4(5)	164.5(6)	209.7(6)
N-C-X / °	179.2(2)	179.5(3)	178.06(17)	176.16(19)	177.7(3)
Fe-N-C _{NcX} / °	171.9(2)	163.2(3)	164.87(15)	169.15(14)	166.73(18)

Table S5. The tetradentate ligand (L) and the spin-state of $[\text{FeL}(\text{NCE})_2]$ discussed.

Ligand	Structural formula	S	Se	B	References
$2\text{MeL}_{\text{quinoline}}$		HS	HS	HS	—
2MeL_{pz}		HS	—	SCO	Inorg. Chem.2017, 56, 12148–12157
L_{Cl}		HS	SCO	SCO	Inorg. Chem. Front., 2018, 00, 1–6
Dibenzyl L		HS SCO	HS	SCO	—
L_1		SCO	—	SCO	Chem. Eur. J. 2012, 18, 5924 – 5934 Dalton Trans., 2015, 44, 20551–20561
2MeL		—	HS SCO	—	Inorg. Chem.2015, 54, 5145–5147
bqen		SCO SCO	SCO SCO	—	Inorg. Chem.2017, 56, 13535–13546
DPEA		SCO	—	—	Inorg. Chem. 1997, 36, 2975-2981
$6\text{-Me}_2\text{-Me}_2\text{uns-penp}$		HS	—	—	Z. Anorg. Allg. Chem. 2012, 2069–2077
L^3		HS	—	—	Inorganica Chimica Acta 337 (2002) 407–419

References

- [1] B. Rieger, A. S. Abu-Surrah. Synthesis of chiral and C₂-symmetric iron(II) and cobalt(II) complexes bearing a new tetradentate amine ligand system. *Journal of Organometallic Chemistry*. **1995**, 497, 73–79.
- [2] J. R. Aldrich-Wright, R. F. Fenton. The synthesis and structural analysis of cis-β-((1,6-di(2'-pyridyl)(2,5-dibenzyl-2,5-diazahexaneO(1,2-diazahexane))(1,2-benzoquinone diimine)) ruthenium(II)) and related complexes. *Journal of Coordination Chemistry*. **2007**, 60, 2015–2034.